Autophagy 10:1, 20–31; January 2014; © 2014 Landes Bioscience

Chromosome 19 open reading frame 80 is upregulated by thyroid hormone and modulates autophagy and lipid metabolism

Yi-Hsin Tseng,[1] Po-Yuan Ke,[2] Chia-Jung Liao,[1] Sheng-Ming Wu,[1] Hsiang-Cheng Chi,[1] Chung-Ying Tsai,[1] Cheng-Yi Chen,[1] Yang-Hsiang Lin,[1] and Kwang-Huei Lin[1,3,*]

[1]Graduate Institute of Biomedical Sciences; College of Medicine; Chang Gung University; Taoyuan, Taiwan; [2]Department of Biochemistry and Molecular Biology, College of Medicine, Chang Gung University, Taoyuan, Taiwan; [3]Department of Medical Research; Chang Gung Memorial Hospital; Taoyuan, Taiwan

Keywords: thyroid hormone, chromosome 19 open reading frame 80, autophagy, lipid droplet, lysosome

Abbreviations: C19orf80, chromosome 19 open reading frame 80; ChIP, chromatin immunoprecipitation; CQ, chloroquine; FFAs, free fatty acids; GFP, green fluorescent protein; HCC, hepatocellular carcinoma; LAMP2, lysosomal-associated membrane protein 2; LDs, lipid droplets; mRFP, monomeric red fluorescent protein; OCR, oxygen consumption rate; PI3K, phosphoinositide 3-kinase; RXR, retinoid X receptor T_3, thyroid hormone 3,3′,5-triiodo-L-thyronine; TG, triglyceride; THR, thyroid hormone receptor; TRE, thyroid hormone response element

The thyroid hormone, T_3, regulates cell growth, differentiation and development through binding to the nuclear thyroid hormone receptor (THR), a member of the steroid/TR superfamily of ligand-dependent transcriptional factors. T_3 modulates lipid metabolism in liver, although the detailed molecular mechanisms are unclear at present. Here, by a microarray analysis, we identified a novel *chromosome 19 open reading frame 80* (*C19orf80*) which was activated by T_3. T_3 stimulation led to upregulation of both mRNA and protein levels of *C19orf80*. Immunofluorescence analysis revealed a vesicle-like pattern of C19orf80 around lipid droplets or within the lysosome-associated compartment in cells. Furthermore, T_3 treatment as well as C19orf80 overexpression specifically activated the autophagic response and lipid metabolism, as observed from lipidated LC3 (LC3-II) and levels of oxygen consumption rate, respectively. Reciprocally, knockdown of C19orf80 obstructed T_3-activated autophagy and lipolysis. Moreover, treatment with autolysosome maturation inhibitors, ammonium chloride and chloroquine, not only suppressed the T_3-activated autophagic process but also lipid metabolism. Our results collectively suggested that T_3 regulates lipid metabolism through a C19orf80-activated autophagic process.

Introduction

The thyroid hormone, 3,3′,5-triiodo-L-thyronine (T_3), exerts a variety of biological effects in nearly all mammalian tissues, in particular, ontogenesis, cell growth, oxygen consumption, and metabolism.[1] The biological activity of T_3 relies on binding to nuclear thyroid hormone receptors belonging to the ligand-dependent transcriptional factor family. Transcriptional regulation of cellular genes by THRs is initiated via interactions with RXR (retinoid X receptor) to form heterodimers that bind to thyroid hormone response elements (TREs) within the promoter regions or introns of target genes.[2]

The liver expresses equal amounts of the thyroid hormone receptors THRA and THRB, implying that T_3 regulates gene expression through transactivation activity.[3] Intriguingly, on the one hand, T_3 promotes lipid catabolism through decreasing total amounts of cholesterol, low-density lipoproteins, and chylomicron particles.[4] On the other hand, T_3 upregulates several lipogenic genes, including low-density lipoprotein receptors, CYP7A1 (cytochrome P450, family 7, subfamily A, polypeptide 1/cholesterol-7α hydroxylase), LIPC (lipase, hepatic), and NR1H3 (nuclear receptor subfamily 1, group H, member 3/liver X receptor-α), promoting lipid biosynthesis.[5-8] Earlier studies indicate that T_3 plays a functional role in maintenance of lipid metabolism in several tissues, particularly liver. Several reports have confirmed that hypothyroidism causes hyperlipidemia, obesity, and nonalcoholic steatohepatitis, which progresses to liver cirrhosis and hepatocellular carcinoma (HCC) development.[9,10] These findings suggest a significant association of malfunction of T_3 and impairment of liver function with pathogenesis of lipid-associated diseases.

Autophagy is a catabolic process involved in bulk degradation of unwanted cytoplasmic components, including aggregated and/or unfolded proteins and damaged organelles.[11] During

*Correspondence to: Kwang-Huei Lin; Email: khlin@mail.cgu.edu.tw
Submitted: 08/29/2012; Revised: 08/09/2013; Accepted: 08/12/2013
http://dx.doi.org/10.4161/auto.26126

the autophagic process, damaged organelles aggregate, and misfolded proteins are sequestered within autophagosomes and delivered to lysosomes for proteolysis and recycling. Recent studies have shown that analogous to the thyroid hormone, autophagy regulates lipid metabolism in liver cells by enhancing catabolism of lipid droplets (LDs), a major storage organelle of excess lipid.[12] In the current study, we focused on investigating the genes regulated by T_3 that are involved in lipid metabolism through the autophagy process.

DNA microarray analysis led to the identification of a novel gene, *chromosome 19 open reading frame 80*, *C19orf80* (also known as hepatocellular carcinoma-associated gene TD26), significantly induced by T_3. *C19orf80* was initially cloned and characterized as a human HCC-associated gene located on chromosome 19p13.2. The *C19orf80* transcript (NM_018687) is composed of 4 exons and encodes a polypeptide of 198 amino acids (NP_061157). Sequence analysis revealed that C19orf80 is a transmembrane protein with a signal peptide and potential myristoylation site at the N-terminal region. Gene expression profiling studies further disclosed that *C19orf80* is regulated by different stimuli [HCV-1b, IFNA (interferon, α), cationic amphiphilic drugs, caloric intake and trichostatin A],[13-17] implying functions in the maintenance of metabolic homeostasis and the regulation of cellular stress response in liver. However, the precise molecular mechanisms by which T_3 regulates *C19orf80* gene expression and the physiological significance of the protein remain to be established.

Here, we propose that T_3 stimulation transactivates *C19orf80* expression, based on the upregulation of *C19orf80* mRNA and protein levels in human hepatoma cell lines. The immunofluorescence assay showed that C19orf80 exhibits a vesicle-like pattern adjacent to the surface of lipid droplets and lysosome-associated expression pattern in cells. In addition, both T_3 treatment and ectopic expression of C19orf80 enhanced autophagic flux and activated the complete autophagy process. Conversely, knockdown of C19orf80 obstructed T_3-mediated activation of autophagy, indicating that T_3 induces the autophagic response through C19orf80. Subsequently, we demonstrated that T_3 and C19orf80 participate in turnover of LDs through autophagy. Our results provided evidence that T_3 activates autophagy via transcriptional regulation of *C19orf80* gene expression, and shed novel insights into the physiological significance of C19orf80 in the modulation of lipid metabolism through regulating LD turnover.

Results

T_3 upregulates *C19orf80* expression in human liver cell lines

DNA microarray analysis was utilized to evaluate gene expression changes in T_3-stimulated cells expressing two independent thyroid hormone receptors, THRA and THRB, HepG2-THRA and HepG2-THRB (**Fig. 1A**), respectively, with the aim of identifying the genes in liver cells regulated by T_3. Comparison of gene expression changes between T_3-stimulated HepG2-THRA and HepG2-THRB cells revealed that *C19orf80*, a HCC-associated gene, is significantly induced by T_3 (**Fig. 1A**, square islet indicated). Using the quantitative reverse transcription-polymerase chain reaction (qRT-PCR) assay, we confirmed that *C19orf80* mRNA is specifically upregulated by T_3 in HepG2-THRA, compared with HepG2-Neo cells expressing empty vector (**Fig. 1B**). Notably, T_3 transactivated *C19orf80* gene expression in a dose- and time-dependent manner (**Fig. 1B**). THRB analogously mediated T_3-induced activation of C19orf80 protein in HepG2 cells (compare upper left and upper right panels in **Fig. 1C**). In contrast, no significant C19orf80 protein was detected in HepG2-Neo cells (**Fig. 1C**, bottom left panel). Our results indicated that T_3-transactivated *C19orf80* gene expression is simultaneously mediated by THRA and THRB. C19orf80 protein was additionally upregulated in Huh7 cells harboring endogenous THRs (**Fig. 1C**, bottom right panel), supporting the theory that T_3 activates *C19orf80* expression through THRs in liver cells. Based on these results, we propose that the thyroid hormone transactivates *C19orf80* gene expression in human liver cells.

T_3-induced *C19orf80* expression depends on the transactivation activity of THR

Next, we established whether TR-mediated transcriptional activation is required for induction of *C19orf80* gene expression by T_3. Sequence analysis revealed several potential thyroid hormone response elements (TREs) within the 3.5-kb genome sequence upstream of the *C19orf80* start codon (**Fig. 1D**). The fragment was subsequently cloned into the pGL3-Luc vector, and the luciferase assay performed. As shown in **Figure 1D**, the 3.5-kb upstream region (construct I, positions –3470~–1) displayed transactivation ability in the presence of T_3. Subsequently, deletion of two TREs (construct II, positions –1527 to ~–1) led to a dramatic decrease in T_3-induced activation of *C19orf80* (**Fig. 1D**). The –3470 to ~–1500 region and serial truncations were further subcloned into pA3tk-Luc vector containing a minimal herpes simplex virus thymidine kinase promoter fragment. Transcriptional activity of construct IV (positions -3020 to ~–1500) was stimulated by T_3, which was reduced in construct V (positions –2900 to ~–1500). This residual T_3 induction indicates minor TRE activity in the –2900~–1500 fragment. A single fragment containing the predicted palindromic ~120 bp sequence (construct VI, positions –3020 to ~–2900) was additionally activated by T_3. Site-directed mutagenesis of the conserved palindromic sequence (**Fig. 1E**) led to impairment of T_3-induced transcriptional activity (**Fig. 1D**). Luciferase assays further supported the presence of a functional TRE in the region upstream of the *C19orf80* sequence. In the in vivo chromatin immunoprecipitation (ChIP) assay, the –3060 to ~–2895 region containing T_3-inducible TRE interacted specifically with immunoprecipitated THR and RXRA (**Fig. 1F**). Our results collectively suggested that the THR-RXRA heterodimer interacts physically with the *C19orf80* upstream element and triggers *C19orf80* transcription upon T_3 activation.

C19orf80 is localized within the endosome/lysosome

To gain insights into the biological function of C19orf80, we initially analyzed its subcellular localization. Immunofluorescence analysis revealed significant C19orf80 expression in HepG2-THRA cells treated with T_3 (**Fig. 2A**, bottom left). In addition, C19orf80 was mainly localized in the cytoplasm, exhibiting a vesicle-like distribution (**Fig. 2A**, bottom

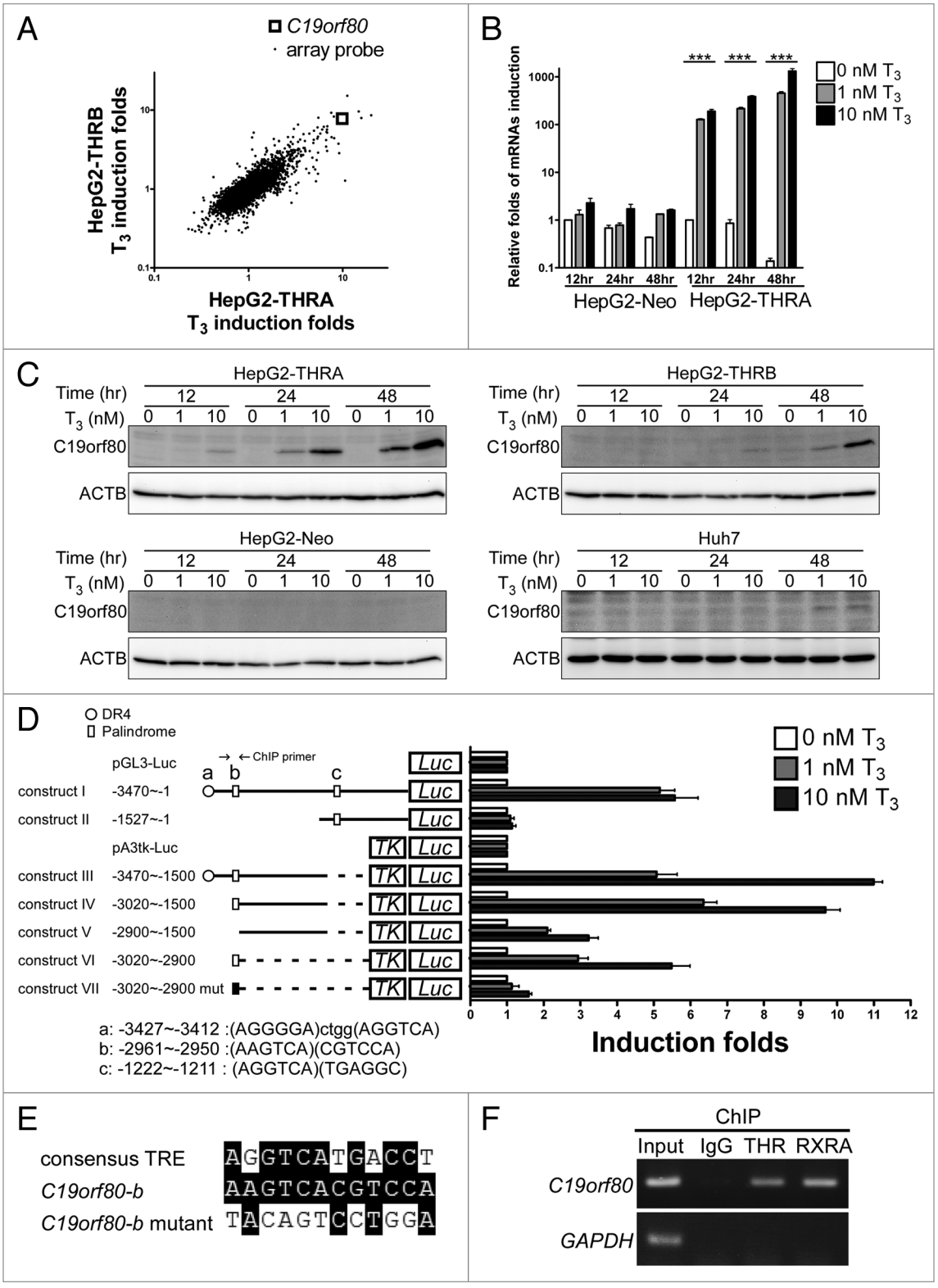

Figure 1. TR upregulates C19orf80 expression in HCC cell lines. (**A**) Affymetrix microarray analysis was performed to determine relative fold induction of T_3 in HepG2-THRA/THRB cells. Each dot represents a specific gene probe. The *C19orf80* tag (220437_at) is indicated. (**B**) qRT-PCR of *C19orf80* mRNA expression levels in HepG2-Neo and HepG2-THRA cells (***$P < 0.001$, n = 3). Error bars: s.e.m. (**C**) Immunoblots of HepG2-THRA, HepG2-THRB, HepG2-Neo and Huh7 cell lysates. (**D**) Schematic representation of the *C19orf80* promoter with potential TRE binding sites (+1, translation start site). Serial deletion or mutated fragments of *C19orf80* 5'-flanking DNA were cloned into pGL3 or pA3tk-luc reporter plasmids, as indicated. T_3 induction fold is presented as mean values ± s.e.m. (n = 3). (**E**) Putative TRE sequences of *C19orf80* are indicated. (**F**) ChIP assay of the *C19orf80* 5′-flanking region (–3060 to ~–2895). The promoter region of *GAPDH* was used as the negative control.

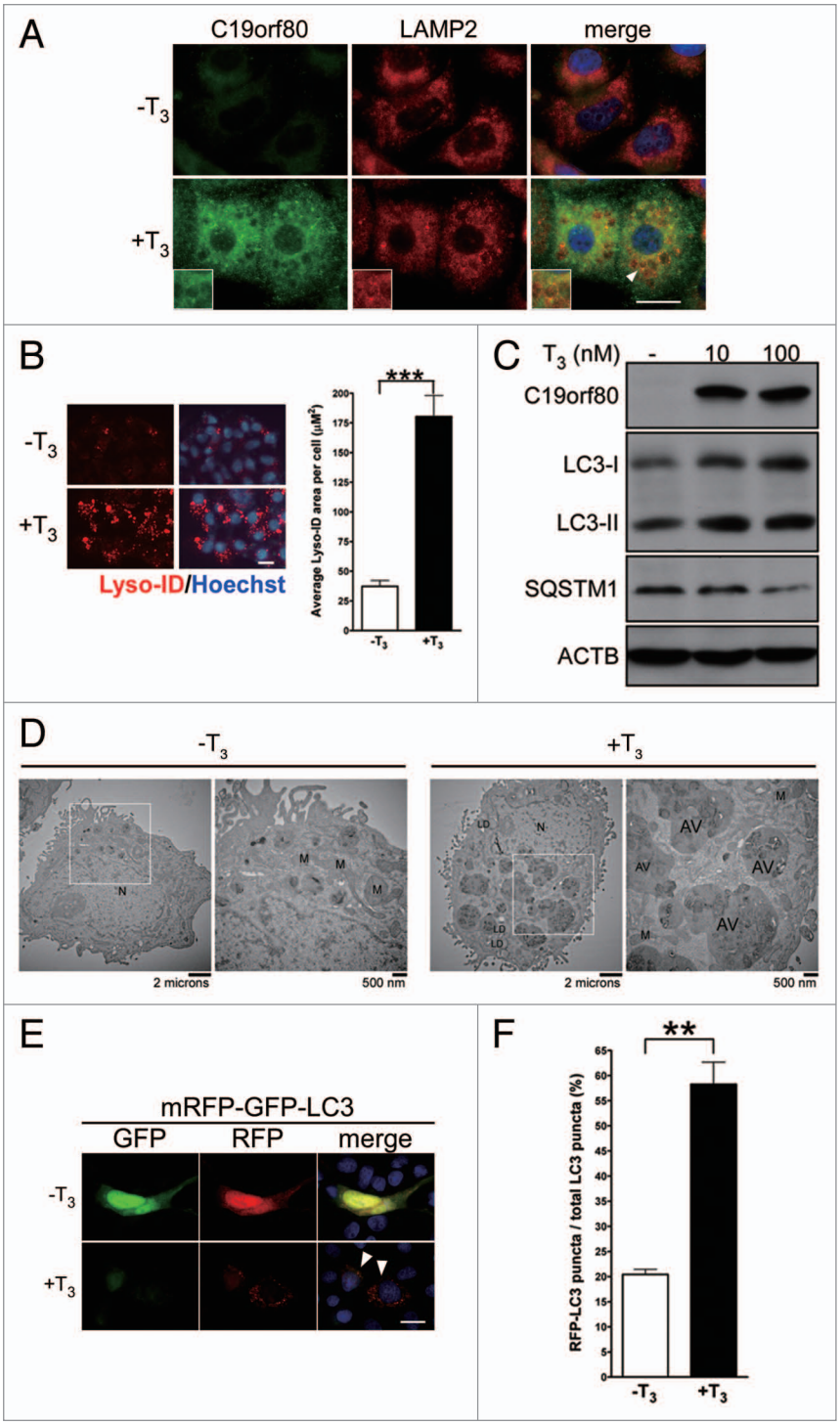

Figure 2. T_3 induces the formation and maturation of autolysosomes. (**A**) Immunofluorescence analysis of C19orf80 with LAMP2 in HepG2-THRA cells (inserts, magnified image of arrowhead indicated). (**B**) Cells were stained with acidotropic dye, Lyso-ID red, to highlight acidic vesicles. Fluorescence signals were captured and analyzed using ImageJ software. (**C**) Immunoblots of HepG2-THRA cell lysates. (**D**) Transmission electron microscopy analysis of HepG2-THRA cells. N, nucleus; M, mitochondria; LD, lipid droplet; AV, autophagic vacuole. (**E**) HepG2-THRA cells were transfected with mRFP-GFP-LC3 expression plasmids overnight. Culture media were replaced for a further 48 h, and fluorescence images captured. (**F**) The percentage of acidic vesicular LC3 (RFP^+/GFP^- signal, arrowhead) was calculated (***$P < 0.001$, **$P < 0.01$, n = 3). Error bars: s.e.m. (**A, B, and E**) Scale bar: 20 μm.

left). Several dot-like structures of C19orf80 were associated with lysosomal-associated membrane protein 2 (LAMP2) and partially with calnexin (CANX), indicating localization at the endosome/lysosome and endoplasmic reticulum (ER) (**Fig. 2A**, arrowhead; **Fig. S1A**), respectively, while C19orf80 was rarely detected in the mitochondria (data not shown). Subcellular fractionation analysis further confirmed that C19orf80 cofractionates with LAMP2 and CANX (**Fig. S1B**, fractions 7 to ~10), consistent with the results presented in **Figure 2A** and **Figure S1A**, respectively. These findings collectively suggested that the C19orf80 signal localizes within the lysosome/endosome and ER-associated compartments.

T_3 promotes the formation and maturation of autophagic vacuoles

Since the endosome/lysosome is responsible for maintenance of cell homeostasis via protease-induced degradation and recycling of the cytosolic content within an acidic environment at pH 4.5–6.0[18] and T_3 regulates lysosomal activity by modulating hydrolytic enzymes or transporter protein,[19-21] we examined whether T_3 affects accumulation of acidic vacuoles in cells. As shown in **Figure 2B**, T_3 treatment of HepG2-THRA cells led to a dramatic increase in the number and size of acidic vacuoles labeled using Lyso-ID red, a specific dye staining the acidophilic compartments in cells. Based on these results, we propose that the thyroid hormone promotes accumulation of acidic organelles, such as endosomes/lysosomes and/or autophagic vacuoles in liver cells.

A decrease in autophagic vacuoles has been reported in the Harderian gland of hypothyroid rats.[22] Accordingly, we examined whether T_3 alters the autophagic response, thus enhancing the accumulation of acidic organelles. After 48 h stimulation with T_3, phosphatidylethanolamine-conjugated microtubule-associated protein 1 light chain 3 (LC3-II) was increased in conjunction with downregulation of SQSTM1 (also known as p62), a cargo receptor that is degraded by the autophagic process (**Fig. 2C**). The data indicate that T_3 activates autophagy to induce the degradative pathway. C19orf80 was concurrently upregulated with activation of autophagy in T_3-stimulated cells (**Fig. 2C**), suggesting association of this gene with the T_3-activated autophagic process. Next, transmission electron microscopy ultrastructural analysis was employed for morphological assessment of activation of

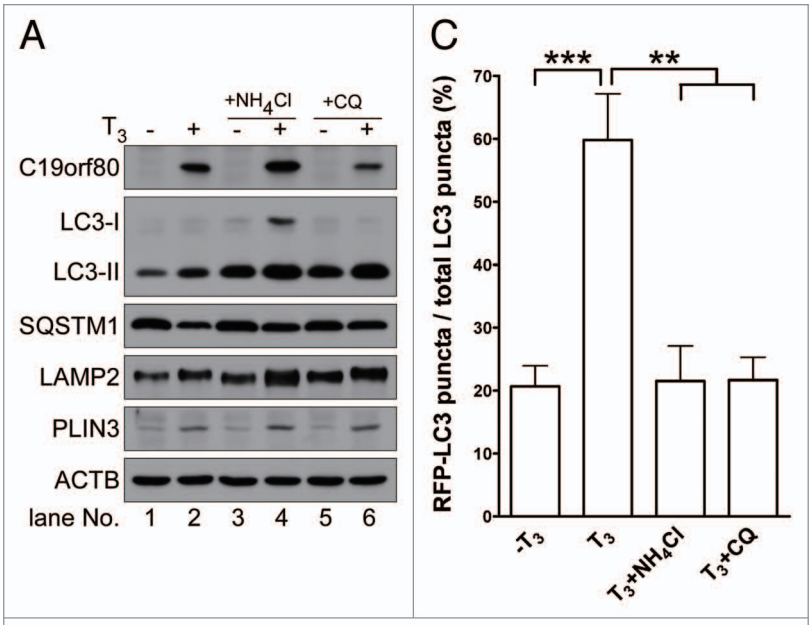

Figure 3. T_3-induced maturation of autolysosomes is blocked by NH_4Cl and CQ. (**A**) HepG2-THRA cells were treated with inhibitors (NH_4Cl: 20 mM, CQ: 50 μM), as indicated, and lysates subjected to immunoblot analysis. (**B**) HepG2-THRA cells were transfected with mRFP-GFP-LC3 overnight. Culture media were treated as for (**A**), and fluorescence images captured. (**C**) The percentage of acidic vesicular LC3 (RFP^+/GFP^- signal) was calculated (***$P < 0.001$, **$P < 0.01$, n = 3). Error bars: s.e.m. Scale bar: 20 μm.

the autophagic response in T_3-treated cells.[23] Significant accumulation of autophagic vacuoles was detected in T_3-stimulated cells, in contrast to mock-treated cells (**Fig. 2D**). To further establish whether T_3 activates autophagy through enhancing the autophagic flux, we analyzed the fluorescence signal of a tandem mRFP (monomeric red fluorescent protein)-GFP (green fluorescent protein)-LC3 reporter in cells stimulated by T_3.[24] Since GFP fluorescence is attenuated by subsequent hydrolysis within lysosomal compartments while RFP remains relatively stable and retains the fluorescence signal within acidic lysosomes,[24] the ratio of GFP and RFP fluorescence can be used to examine whether activated autophagosomes proceed to the fusion step with lysosomes, forming an acidic autolysosome. Upon culture of cells in T_3-depleted medium, GFP and RFP signals of the mRFP-GFP-LC3 tandem reporter exhibited homogenous distribution throughout the cytoplasm and nucleus (**Fig. 2E**, upper row). Following T_3 stimulation, the RFP (but not GFP) signal of the mRFP-GFP-LC3 tandem reporter was concentrated as a punctate structure (RFP^+/GFP^-, hereafter designated "RFP-LC3 puncta") (**Fig. 2E**, bottom row). In quantification analysis, the ratio of the number of RFP-LC3 puncta to total LC3 puncta structures in cells was increased in T_3-treated cells, compared with that in cells depleted of T_3 (**Fig. 2F**).

The T_3-induced LC3-II level was further increased in cells treated with ammonium chloride (NH_4Cl) and chloroquine (CQ), two pharmacological inhibitors that interfere with autolysosome maturation (**Fig. 3A**, lanes 2 vs. 4 and 6).[25] In addition, degradation of SQSTM1 in T_3-treated cells was inhibited (**Fig. 3A**, lanes 2 vs. 4 and 6). NH_4Cl and CQ treatment restored the GFP fluorescence signal of the mRFP-GFP-LC3 tandem reporter (**Fig. 3B**), resulting in a decrease in the ratio of RFP-LC3 puncta to total LC3 punctate structures in cells stimulated with T_3 (**Fig. 3C**). Our results indicate that the thyroid hormone activates complete autophagy in liver cells.

C19orf80 activates the autophagy process through to complete autolysosome maturation

In view of the findings that T_3 simultaneously upregulates C19orf80 as well as autophagy, and C19orf80 localizes with lysosomal compartments in cells (**Fig. 2A and C**), we further investigated whether enhancing C19orf80 expression in cells induces autophagy in a similar manner to that in cells stimulated by T_3. Ectopic expression of C19orf80 resulted in accumulation of acidic vacuoles in cells (**Fig. 4A**), analogous to T_3-stimulated cells (**Fig. 2B**). In addition, overexpression of C19orf80 induced an increase in the LC3-II level and decrease in SQSTM1 in cells (**Fig. 4B**, lane 2), compared with empty vector-transfected cells (lane 1). Treatment with NH_4Cl and CQ led to further accumulation of C19orf80-induced LC3-II and suppressed degradation of SQSTM1 (**Fig. 4B**, lane 3 vs. 4, lane 5 vs. 6, respectively). Consistent with this finding, the amount of RFP-LC3 punctate structures was increased in C19orf80-overexpressing cells transfected with the mRFP-GFP-LC3 reporter (**Fig. 4C and D**). Clearly, C19orf80 expression is sufficient to activate the complete autophagy process in liver cells.

T_3 activates the complete autophagy process through C19orf80 gene expression

To further clarify whether C19orf80 is required for T_3-induced autophagy, we examined the effects of C19orf80

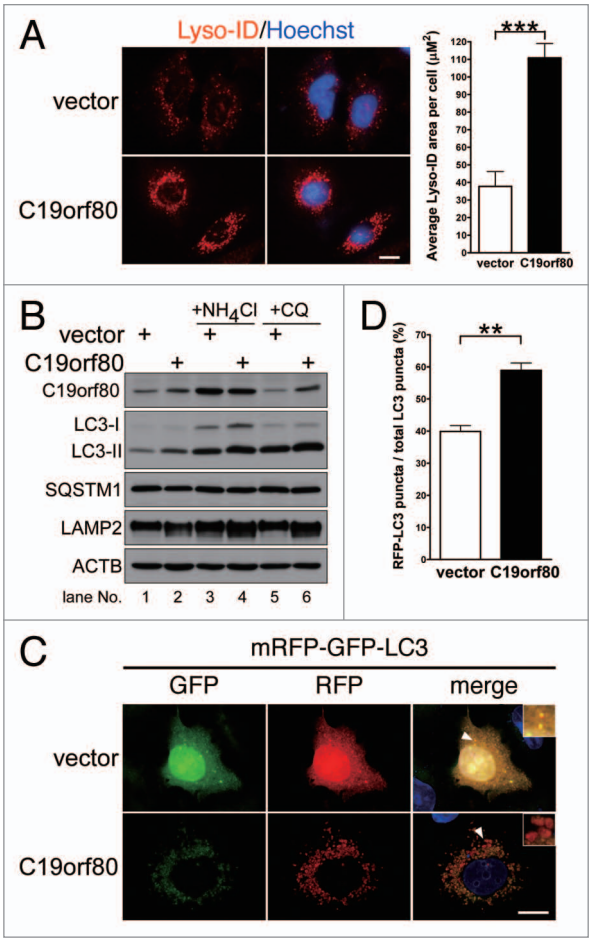

Figure 4. C19orf80 induces an increase in acidic vesicles and promotes autophagy (**A**) Lyso-ID staining of Huh7-C19orf80 cells. Fluorescence signals were analyzed. (**B**) Immunoblots of Huh7-C19orf80 cell lysates. Cells were pretreated with inhibitors (NH_4Cl: 20 mM, CQ: 50 μM) for 24 h. (**C**) mRFP-GFP-LC3 expression plasmids were transfected into C19orf80-overexpressing Huh7 and control cells for 72 h. (**D**) The percentage of acidic vesicular LC3 (RFP$^+$/GFP$^-$ signal, arrowhead) was calculated (***P < 0.001, **P < 0.01, n = 3). Error bars: s.e.m. (**A and C**) Scale bar: 20 μm.

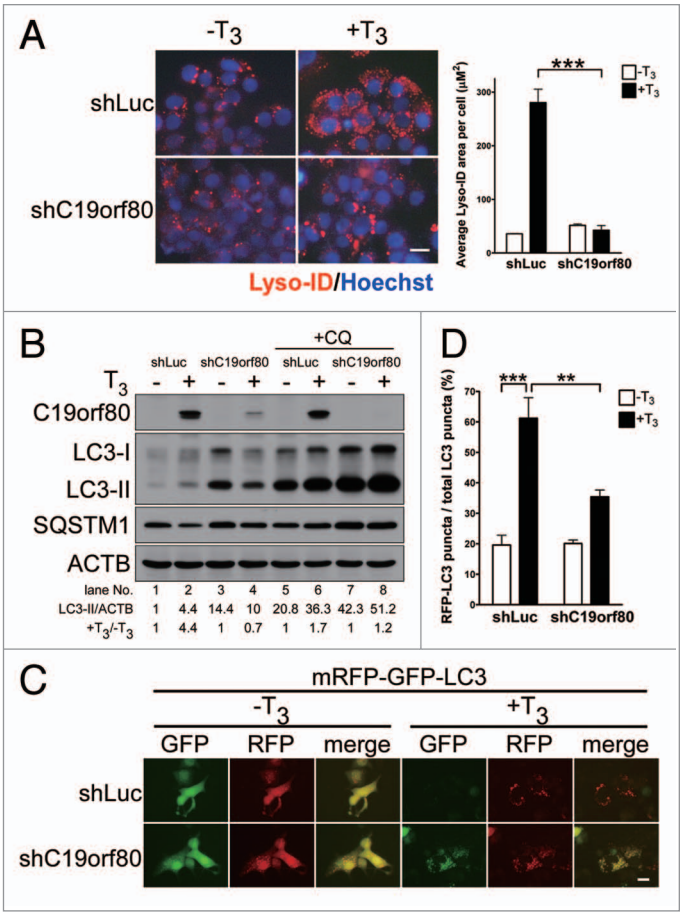

Figure 5. C19orf80 knockdown compromises T_3-induced autophagy. (**A**) C19orf80 knockdown and cognate control HepG2-THRA cells were stained with Lyso-ID. Fluorescence signals were captured and analyzed. (**B**) Immunoblots of C19orf80 knockdown and control cells. Cells were pretreated with CQ (50 μM) for 24 h. Relative fold of T_3-induced LC3-II lipidation is presented (LC3-II/ACTB, $+T_3/-T_3$). (**C**) mRFP-GFP-LC3 expression plasmids were transfected into C19orf80 knockdown and control cells overnight. Culture media were replaced for a further 48 h, and fluorescence images captured. (**D**) The percentage of acidic vesicular LC3 (RFP$^+$/GFP$^-$ signal) was calculated (***P < 0.001, **P < 0.01, n = 3). Error bars: s.e.m. Scale bar: 20 μm.

knockdown on the T_3-induced increment of acidic vacuoles, LC3-II accumulation, and SQSTM1 degradation. Knockdown of C19orf80 by itself did not affect acidic vesicle formation upon culture in T_3-depleted serum. However, after T_3 treatment, C19orf80 knockdown cells exhibited fewer lysosomes, compared with control cells containing large amounts of Lyso-ID-labeled lysosome (**Fig. 5A**). Moreover, the T_3-activated fold of LC3-II level was reduced (comparing the ratio index below lanes 2 and 4 in **Fig. 5B**) and the SQSTM1 level was increased in cells with a knockdown of C19orf80. Importantly, interference with T_3-induced C19orf80 expression via gene silencing abolished the increase in LC3-II by CQ (comparing the ratio index below lanes 6 and 8 in **Fig. 5B**). Furthermore, the T_3-stimulated ratio of RFP-LC3 puncta to total LC3 punctate structures of the mRFP-GFP-LC3 tandem reporter was decreased following C19orf80 knockdown (**Fig. 5C and D**). It should be noted that silencing of C19orf80 gene expression partially rescued the GFP fluorescence signal of the mRFP-GFP-LC3 tandem reporter and C19orf80 was cofractionated with LAMP2 as well as LC3-II and SQSTM1 in the T_3-treated cells (**Fig. 5D** and **Fig. S1B**, respectively). These results imply that C19orf80 is targeted to autophagic vacuoles, particularly acidic autolysosomes, and plays a role in autolysosome maturation to regulate T_3-activated autophagy. Based on these data, we propose that thyroid hormone activates the autophagy process through C19orf80 upregulation.

T_3-induced C19orf80 associates with lipid droplets

Since autophagy regulates lipid metabolism by enhancing LD catabolism, we addressed whether T_3-induced autophagy via C19orf80 participates in lipid catabolism. Using immunofluorescence analysis, we initially showed that C19orf80 colocalizes with PLIN3 (perilipin 3, a LD-associated protein) (**Fig. 6A**, bottom row). Moreover, endogenous C19orf80 in cells with T_3 stimulation or ectopically expressing

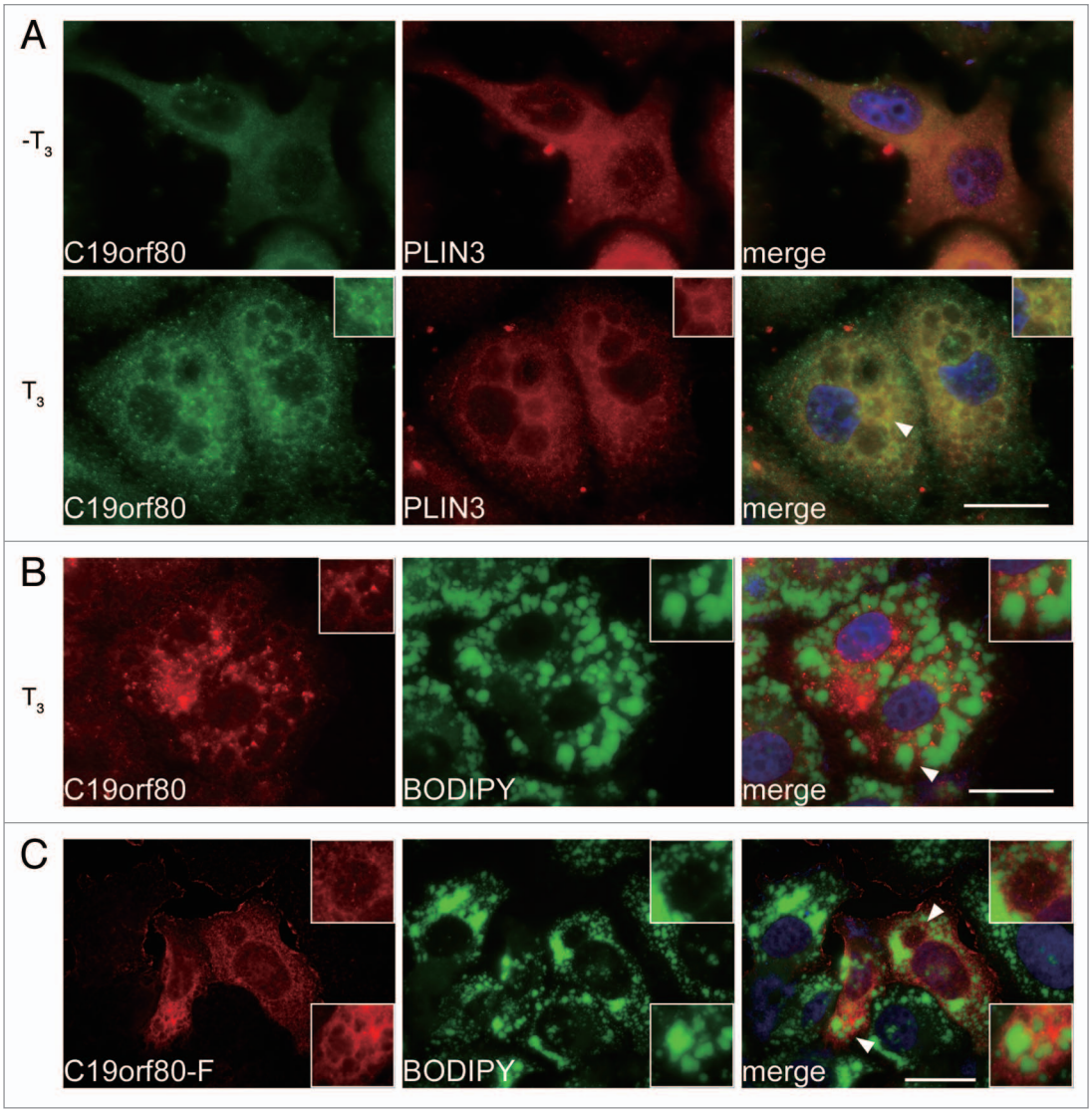

Figure 6. T_3-induced C19orf80 is associated with lipid droplets. (**A**) Immunofluorescence analysis of C19orf80 with PLIN3 in HepG2-THRA cells. BODIPY staining of T_3-induced C19orf80 in HepG2-THRA cells (**B**) or FLAG-tagged C19orf80 in Huh7 cells (**C**). The insert shows magnified image of region indicated by arrowhead. Scale bar: 20 μm.

FLAG-C19orf80 exhibited localization signals on the surface of LDs labeled with the lipophilic dye, BODIPY 493/503 (**Fig. 6B**, magnification insert and **Fig. 6C**, lower insert, respectively). Subcellular fractionation additionally disclosed that a proportion of PLIN3 cofractionates with C19orf80 (**Fig. S1B**, fractions 2 and 3). Immunofluorescence analysis of FLAG-C19orf80 in HepG2-THRA cells further confirmed that C19orf80 was partially associated with PLIN2 (perilipin 2, a known protein localized on the surface of LDs) and BODIPY staining (**Fig. S2A and S2B**, magnified image, arrowhead). The distinct distribution of C19orf80 was in accordance with subcellular fractionation that C19orf80 exists in both the light (**Fig. S1B**, fractions 2–3, with PLIN3) and heavy (**Fig. S1B**, fractions 7 to ~10, with LAMP2 and LC3-II) fractions. Our findings indicated that a portion of thyroid hormone-induced C19orf80 associates with LDs.

T_3-induced C19orf80 participates in lipid metabolism

To establish whether T_3-activated autophagy facilitates degradation and catabolism of LDs in liver cells, we initially treated T_3-stimulated cells with NH_4Cl and CQ, with a view to establish whether interference with the complete autophagy process restores LD expression. As shown in **Figure 7A**, T_3 stimulation led to an increase in LDs, presumably through transcriptional activation of lipogenic genes.[5-8] Treatment with NH_4Cl and CQ further upregulated T_3-induced LC3-II expression (**Fig. 3A**) as well as LD levels (**Fig. 7A**). The intracellular triglyceride (TG) content in T_3-treated cells accumulated in a similar manner (**Fig. 7B**). The etomoxir-inhibited oxygen consumption rate (OCR; see Materials and Methods), an indirect measurement of free fatty acids (FFAs) oxidation in cells, was enhanced upon T_3 stimulation (**Fig. 7C**), implying that T_3 accelerates LD catabolism to FFAs via autophagy. In contrast,

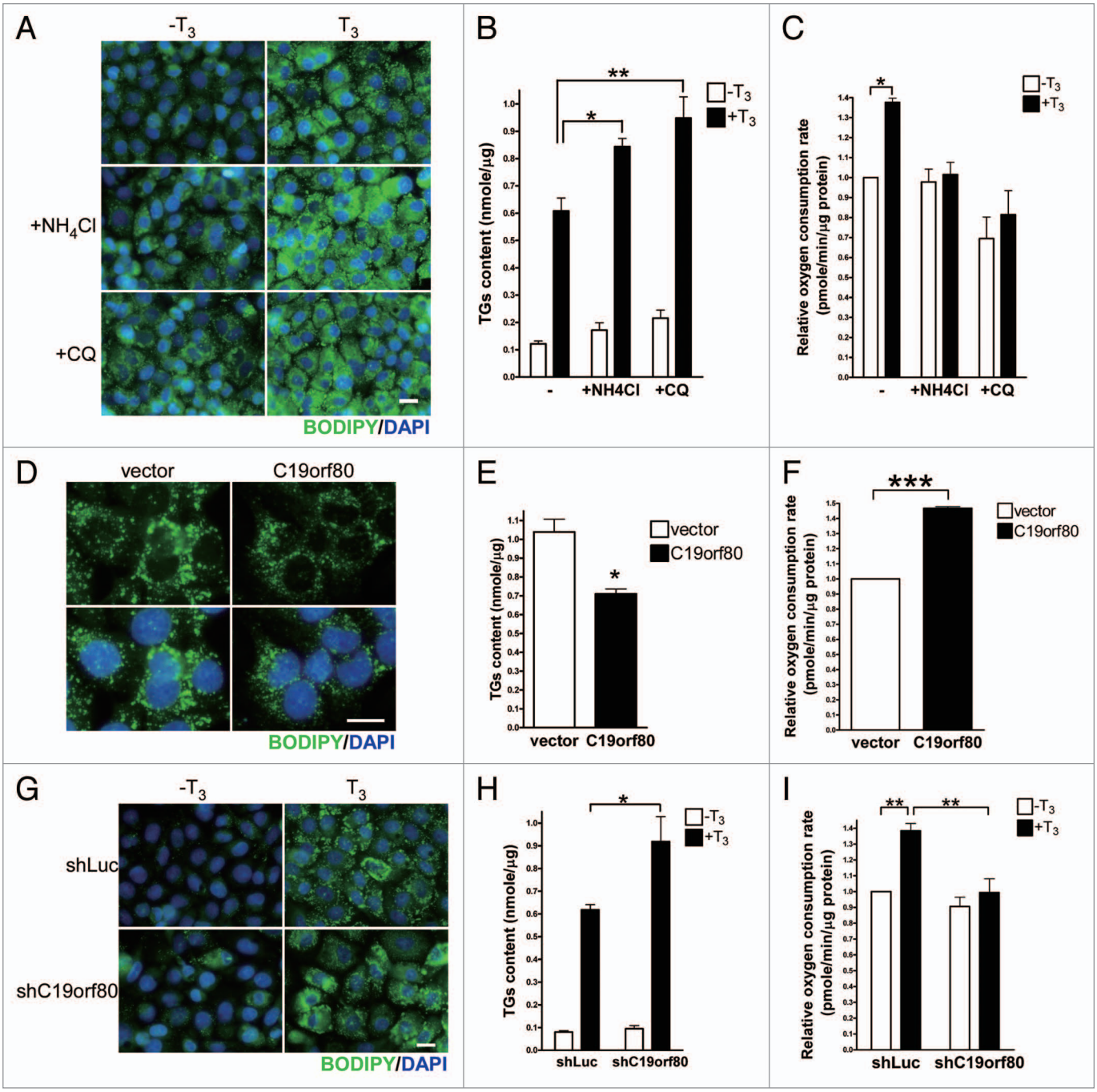

Figure 7. T_3-induced C19orf80 is associated with lipid metabolism. (**A–C**) HepG2-THRA cells were cultured in the absence or presence of 10 nM T_3 for 24 h. Acidic inhibitors were added for a further 24 h, as indicated. (**D–F**) Huh7-C19orf80 and vector control cells were plated for 48 h. (**G-I**) C19orf80 knockdown and cognate control HepG2-THRA cells were cultured in the absence or presence of 10 nM T_3 for 48 h. Lipid droplets were stained with BODIPY (**A, D, and G**), and triglyceride (TG nmole/μg) (**B, E, and H**) and oxygen consumption rate (pmole/min/μg protein) (**C, F** and **I**) detected. (***P < 0.001, **P < 0.01, *P < 0.05 n = 3). Error bars: s.e.m. Scale bar: 20 μm.

inhibition of T_3-induced complete autophagy by NH_4Cl and CQ diminished the T_3-induced fold change of OCR (**Fig. 7C**). Furthermore, treatment of T_3-stimulated cells with NH_4Cl and CQ enhanced the oleic acid-induced LD number and size (**Fig. S3A and S3C**). However, the number and size of LDs were not affected by NH_4Cl and CQ in T_3-stimulated cells treated with palmitic acid, a saturated FFA that is poorly converted to TG and enriched in LDs (**Fig. S3B and S3D**). These results indicate that the T_3-activated autophagic response triggers a proteolytic process to degrade LDs.

Overexpression of C19orf80 led to a reduction in the number and size of LDs as well as TG content, whereas the oxygen consumption was upregulated (**Fig. 7D–F**; **Fig. S3E and S3F**), indicating that T_3 promotes LD catabolism through the

C19orf80-induced autophagy process. Moreover, knockdown of C19orf80 in T_3-treated cells increased the LD number and size, and TG levels and reduced the OCR (**Fig. 7G–I**; **Fig. S3G and S3H**), further confirming that C19orf80 is required for T_3-activated lipophagy. In keeping with this finding, C19orf80 was localized on the surface of LDs and associated with PLIN3 (**Fig. 6**; **Fig. S1B**), supporting the theory that C19orf80 participates in the degradation of LDs. Taken together, we propose that C19orf80 functions in thyroid hormone-regulated lipid metabolism through promoting the breakdown of LDs.

Discussion

Autophagy is activated to modulate intracellular metabolites, such as lipids, for the successful maintenance of cell homeostasis. Analogous to the autophagic response, T_3 functions as a key regulator in the modulation of lipid metabolism. However, the issue of whether T_3 regulates lipid metabolism through effects on the autophagy pathway remains to be established. Recently, Sinha and coworkers showed that T_3 activates autophagy to enhance β-oxidation of FFAs, implying that T_3 stimulates a new route to regulate hepatic lipid metabolsim.[26] However, the molecular mechanisms by which T_3 induces autophagy and modulates β-oxidation of FFAs remain unclear. In the current study, we demonstrated that T_3 activates complete autophagy through to autolysosome maturation via transactivation of *C19orf80* in human hepatoma cell lines. Ectopic expression of C19orf80 in liver cells was sufficient to trigger the entire autophagic response. Conversely, knockdown of endogenous C19orf80 suppressed T_3-induced autophagy. Moreover, both T_3 and C19orf80 promoted catabolism of LDs, as evident from the increased levels of oxygen consumption. Our results suggest that T_3 regulates lipid metabolism via a C19orf80-mediated autophagic response.

The cellular function of C19orf80 is largely unknown at present. Initially, we focused on establishing the cellular localization of C19orf80. Immunofluorescence microscopy revealed that T_3-induced C19orf80 forms small punctate vesicular structures of variable sizes. Moreover, C19orf80 associated with LAMP2, indicative of endosomal and lysosomal distribution. Several lines of evidence support a role of T_3 in lysosomal activity via regulation of hydrolytic enzymes or transporter protein.[19-21] T_3 has additionally been shown to upregulate several lipogenic genes to promote biosynthesis of lipids.[5-8] Lipid droplets are surrounded by C19orf80, implying a functional correlation of endosomes/lysosomes with lipid vacuoles. Autophagy is a characteristic of cytoplasmic vacuolation.[27] Notably, autophagic vacuoles are reduced in the Harderian gland of hypothyroid rats.[22] In our experiments, LAMP2, an important factor for autolysosome fusion,[28] was induced by T_3 and associated with C19orf80, consistent with the theory that T_3 is involved in vacuolization and degradation. Accordingly, we postulated that C19orf80 functions in lysosome activity, focusing on T_3-induced autophagic flux. Our results clearly indicated that T_3 is involved in the autophagy pathway, consistent with a recent study.[26] Furthermore, C19orf80 appears to participate in the autophagic flux and lipid metabolism.

Rapamycin, a mechanistic target of rapamycin (MTOR) inhibitor, reverses the inhibitory effects of excess amino acids on autophagic proteolysis and autophagic sequestration in rat hepatocytes.[29] The MTOR pathway regulates the ULK1 kinase complex and inhibits the initial step of autophagosome formation.[30] Several hormones have been shown to modulate autophagy via the MTOR pathway. For instance, glucocorticoid hormones induce a stress response gene, *DDIT4* (*DNA-damage-inducible transcript 4*), to repress MTOR signaling and promote autophagy in lymphocytes and osteocytes.[31,32] Moreover, serum deficiency induces both autophagy and apoptosis in mammary epithelial cells. Meanwhile, another study has reported that the autophagy pathway is suppressed by IGF1 [insulin-like growth factor 1 (somatomedin C)] and EGF (epidermal growth factor), but activated by 17β-estradiol and progesterone.[33] In the midgut and fat body of *Drosophila* larvae, ecdysone triggers programmed autophagy by downregulating the phosphoinositide 3-kinase (PtdIns3K) pathway during the final larval stage.[34] T_3 additionally stimulates the AKT1-MTOR-RPS6KB pathways in myocytes, fibroblasts, and hepatoma cells.[35-38] T_3-induced AKT1-MTOR-RPS6KB kinase signaling and cardiac hypertrophy are prevented by rapamycin, indicating that hypertrophy occurs as a consequence of aberrant regulation of protein synthesis and autophagic degradation.[35,37] In fibroblasts, T_3 induces rapid activation of AKT1 and its nuclear translocation, leading to phosphorylation of nuclear MTOR.[36] In HepG2 cells, T_3 stimulates protein expression of the lipogenic transcription factor, SREBF1 (sterol regulatory element binding transcription factor 1), without affecting *SREBF1* mRNA abundance.[38] This post-transcriptional modulation is suggested to be dependent on PtdIns3K-AKT1-MTOR pathway activation, since a PtdIns3K inhibitor effectively abolishes the stimulatory effect of T_3. In contrast, the effect of T_3 on SREBF1 is further enhanced by rapamycin, suggesting negative feedback of the MTOR target, RPS6KB, on the PtdIns3K-AKT1 pathway.[38] The results suggest that T_3 also inhibits autophagy via enhancement of the MTOR pathway. Conversely, TP53INP2 (tumor protein p53 inducible nuclear protein 2/ diabetes- and obesity-regulated), which is T_3-activated and serves as a nuclear cofactor of THRs, is reported to physically interact with LC3 to stimulate autophagosome formation and accelerate degradation of stable proteins.[39-41] This discrepancy in regulation may stem from innate differences in cell characteristics or integrated signals of the cell environment. For instance, lysosome enzymes are induced by T_3 in liver cells, but are not affected by T_3 in heart and kidney.[20]

As specified above, *C19orf80* levels are regulated by various factors, including HCV-1b, IFNA, cationic amphiphilic drugs, caloric intake and trichostatin A.[13-17] Interestingly, these targeting factors are essentially involved in the lysosomal or autophagy pathway. For instance, hepatitis C virus infection induces autophagy and is inhibited by autophagic inhibitors.[23] The antiviral response of IFNA also induces autophagy.[42] Cationic drugs inhibit lysosomal activity and trigger autophagic vacuolization.[43] Extended longevity via caloric restriction and

resveratrol has additionally been associated with autophagy induction.[44,45] Conversely, transverse aortic constriction-induced autophagy is abolished by the histone deacetylase inhibitor, trichostatin A.[46] It is possible that these agents act through C19orf80, utilizing lysosomal activity to modulate the autophagy pathway, which would provide an explanation for T_3-regulated liver physiology and pathogenesis.

In summary, we have shown that *C19orf80*, a liver-specific gene, is potently induced by T_3 at the transcriptional level. T_3-induced C19orf80 localizes onto LDs and may targets the LDs to autophagic degradation, thus regulating lipid metabolism.

Materials and Methods

Cell cultures

Human hepatoma cell lines, HepG2 and Huh7, were maintained in Dulbecco's modified Eagle's medium supplemented with 10% (v/v) fetal bovine serum in a humidified atmosphere under 5% CO_2. T_3 depletion (Td) serum was prepared by depletion of T_3 with AG 1-X8 resin (Bio-Rad, 140-1451), as described previously.[47]

qRT-PCR

Total RNA was extracted from cells using TRIzol (Invitrogen, 10296-028) as previously described.[48] Subsequently, cDNA was synthesized using the SuperscriptII kit for RT-PCR (Invitrogen, 18064-014). qRT-PCR was conducted in a 15-μl reaction mixture containing 50 nM forward and reverse primers, 1 × SYBR Green reaction mix (Applied Biosystems, 4309155), and 3.2 nM template, as described previously.[48] The sequences of primers for quantitative real-time PCR are listed in **Table S1**.

SDS-PAGE and immunoblot analysis

Cell lysates were harvested as previously described.[48] The equal amounts of protein were resolved by 12% SDS-PAGE, and the gel was transferred to nitrocellulose membrane. The membrane was blocked in 5% (w/v) nonfat dried milk for 1 h and incubated with primary antibodies at 4 °C overnight. After further washing, the membrane was incubated with the appropriate secondary antibodies for 2 h at room temperature. Immune complexes were visualized with chemiluminescence using an ECL detection kit (Amersham, RPN2232), as described in a previous report.[48]

Fluorescence image analysis

For immunofluorescence analysis, cells were fixed with 4% paraformaldehyde, blocked and incubated with the primary and corresponding secondary antibodies. Images were acquired using Carl Zeiss Axiovert 200M microscope and AxioVision Rel. 4.7 software. Lysosomal vesicles were highlighted with Lyso-ID red. Fluorescence images were captured and quantified using imageJ software (Version 1.43s, National Institutes of Health). The average Lyso-ID areas were measured from the randomly selected fields containing more than 100 cells, and average pixels converted to square micrometers. For quantification of acidic autophagic vesicles, cells were transfected with mRFP-EGFP-LC3 fusion protein-expressing plasmid.[24] After T_3 and/or inhibitor treatment, percent of acidic aggregates (red dots/total dots) per cell were counted. Lipid droplets were fixed and stained with BODIPY 493/503 for 20 min. Fluorescence images were captured under a GE Healthcare's IN Cell Analyzer 1000. The number and size of lipid droplets were quantified using IN Cell Investigator software.

Antibodies and reagents

The following antibodies or reagents were used: Mouse polyclonal C19orf80 (Abnova, H00055908-B01), rabbit polyclonal LC3 (Cell Signaling Technology, 2775), mouse monoclonal SQSTM1 (Santa Cruz Biotechnology, sc-28359), rabbit monoclonal LAMP2 (Epitomics, 3660-1), rabbit monoclonal CANX (Epitomics, 2692-1), rabbit monoclonal PLIN2 (Epitomics, 3293-1), mouse monoclonal FLAG (Sigma-Aldrich, F3165), mouse monoclonal ACTB (Chemicon, MAB1501R), goat polyclonal PLIN3 (Santa Cruz Biotechnology, sc-14723) and rabbit polyclonal RXRA (Santa Cruz Biotechnology, sc-553). Mouse monoclonal antibody against TR (C4) was a gift from Sheue-yann Cheng (National Cancer Institute). AG 1-X8 (Bio-Rad, 140-1451), T_3 (Sigma-Aldrich, T2752), chloroquine (Santa Cruz Biotechnology, sc-205629), ammonium chloride (Merck, 101145), Lyso-ID (Enzo Life Sciences, ENZ-51005), oleic acid (Sigma-Aldrich, O1008), palmitic acid (Sigma-Aldrich, P5585), BODIPY 493/503 (Invitrogen, D-3922) and etomoxir sodium salt (Sigma-Aldrich, E1905).

Plasmid construction

To construct the various *C19orf80* promoter reporter plasmids, fragments of the *C19orf80* upstream element (–3470 to –1, +1 corresponding to the AUG initiation site) and truncation mutants were amplified by PCR, and subcloned into pGL3-Luc or pA3tk-Luc vector. For overexpression, *C19orf80* cDNA was amplified by PCR and inserted into the pcDNA3.1 (Invitrogen, V875-20) and p3xFLAG-CMV-14 vectors (Sigma, E7908). The sequences of primers used in this study are listed in **Table S1**.

Reporter assay and ChIP assay

HepG2-THRA cells were transfected with the indicated *C19orf80* promoter reporters using Turbofect reagent (Thermo Fisher Scientific, R0531). Treated cells were harvested for the determination of firefly luciferase activity (Promega, E1960).

The ChIP assay was performed as previously described.[49] Briefly, THR- or RXRA-binding DNA was immunoprecipitated with the corresponding antibody, and the immunoprecipitated DNA fragments were amplified using specific primer sets targeted to the *C19orf80* TRE. The promoter region of *GAPDH* (*glyceraldehyde-3-phosphate dehydrogenase*), which does not contain conserved TRE, was used as the negative control.

Overexpression and knockdown of C19orf80

For stable overexpression of C19orf80, Huh7 cells were transfected with pcDNA3.1- *C19orf80* and selected with hygromycin (50 μg/ml; Sigma-Aldrich, H7772) for two weeks. Then the surviving cells were pooled and cultured as previously described.[21] For overexpression of FLAG-tagged C19orf80, cells were transfected with p3xFLAG-CMV-14-*C19orf80*. To knock down endogenous C19orf80, HepG2-THRA cells were transfected with the lentiviral short hairpin (sh) RNA-expressing plasmid as described previously.[21] The pLKO.1 shLuc

and pLKO.1 shC19orf80-expressing vectors were purchased from the National RNA Interference Core Facility (Institute of Molecular Biology, Academia Sinica, Taipei, Taiwan). Clone TRCN0000072243 was for shLuc, and TRCN0000162915 for shC19orf80.

Triglyceride content and oxygen consumption analysis

The cellular triglyceride content was measured using an adipogenesis assay kit (BioVision, K610-100). For indirect monitoring of fatty acid oxidation, the extracellular oxygen consumption rate was measured accompanied with the β-oxidation inhibitor (etomoxir). Briefly, cells were seeded in Seahorse XF24 microplates under desired growth conditions. Growth media were replaced with assay media (2% serum without sodium bicarbonate) without CO_2 supplied for 1 h. Total oxygen consumption rate (OCR_{total}) was initially measured by Seahorse Extracellular Flux XF24 analyzer and basal respiration ($OCR_{respiration}$) was subsequently measured by adding etomoxir (50 μM). The value of OCR_{total} – $OCR_{respiration}$ (pmole/min/μg protein) was suggestive of oxygen consumption for β-oxidation.

Statistical analysis

Values are expressed as means ± s.e.m. of at least three experiments. Statistical analysis of data was performed with the Student *t* test or one-way ANOVA. $P < 0.05$ was considered significant.

Disclosure of Potential Conflicts of Interest

No potential conflicts of interest were disclosed.

Acknowledgment

We are indebted to Tamotsu Yoshimori (pmRFP-GFP-LC3; Osaka University, Osaka, Japan) for providing the plasmids used in this study. This work was supported by grants from Chang Gung Memorial Hospital, Taoyuan, Taiwan (CMRPD 170092) and from the National Science Council of the Republic of China (NSC 96-2320-B-182-007, NMRP 140513).

Supplemental Materials

Supplemental materials may be found here:
www.landesbioscience.com/journals/autophagy/article/26126

References

1. Yen PM. Physiological and molecular basis of thyroid hormone action. Physiol Rev 2001; 81:1097-142; PMID:11427693
2. Dong H, Yauk CL, Rowan-Carroll A, You SH, Zoeller RT, Lambert I, Wade MG. Identification of thyroid hormone receptor binding sites and target genes using ChIP-on-chip in developing mouse cerebellum. PLoS One 2009; 4:e4610; PMID:19240802; http://dx.doi.org/10.1371/journal.pone.0004610
3. Chamba A, Neuberger J, Strain A, Hopkins J, Sheppard MC, Franklyn JA. Expression and function of thyroid hormone receptor variants in normal and chronically diseased human liver. J Clin Endocrinol Metab 1996; 81:360-7; PMID:8550778; http://dx.doi.org/10.1210/jc.81.1.360
4. Duntas LH. Thyroid disease and lipids. Thyroid 2002; 12:287-93; PMID:12034052; http://dx.doi.org/10.1089/10507250252949405
5. Hansson P, Valdemarsson S, Nilsson-Ehle P. Experimental hyperthyroidism in man: effects on plasma lipoproteins, lipoprotein lipase and hepatic lipase. Horm Metab Res 1983; 15:449-52; PMID:6642415; http://dx.doi.org/10.1055/s-2007-1018751
6. Hashimoto K, Matsumoto S, Yamada M, Satoh T, Mori M. Liver X receptor-alpha gene expression is positively regulated by thyroid hormone. Endocrinology 2007; 148:4667-75; PMID:17628006; http://dx.doi.org/10.1210/en.2007-0150
7. Ness GC, Pendleton LC, Li YC, Chiang JY. Effect of thyroid hormone on hepatic cholesterol 7 alpha hydroxylase, LDL receptor, HMG-CoA reductase, farnesyl pyrophosphate synthetase and apolipoprotein A-I mRNA levels in hypophysectomized rats. Biochem Biophys Res Commun 1990; 172:1150-6; PMID:2123100; http://dx.doi.org/10.1016/0006-291X(90)91568-D
8. Pandak WM, Heuman DM, Redford K, Stravitz RT, Chiang JY, Hylemon PB, Vlahcevic ZR. Hormonal regulation of cholesterol 7alpha-hydroxylase specific activity, mRNA levels, and transcriptional activity in vivo in the rat. J Lipid Res 1997; 38:2483-91; PMID:9458272
9. Loria P, Carulli L, Bertolotti M, Lonardo A. Endocrine and liver interaction: the role of endocrine pathways in NASH. Nat Rev Gastroenterol Hepatol 2009; 6:236-47; PMID:19347015; http://dx.doi.org/10.1038/nrgastro.2009.33
10. Pearce EN. Update in lipid alterations in subclinical hypothyroidism. J Clin Endocrinol Metab 2012; 97:326-33; PMID:22205712; http://dx.doi.org/10.1210/jc.2011-2532
11. Ravikumar B, Sarkar S, Davies JE, Futter M, Garcia-Arencibia M, Green-Thompson ZW, Jimenez-Sanchez M, Korolchuk VI, Lichtenberg M, Luo S, et al. Regulation of mammalian autophagy in physiology and pathophysiology. Physiol Rev 2010; 90:1383-435; PMID:20959619; http://dx.doi.org/10.1152/physrev.00030.2009
12. Singh R, Kaushik S, Wang Y, Xiang Y, Novak I, Komatsu M, Tanaka K, Cuervo AM, Czaja MJ. Autophagy regulates lipid metabolism. Nature 2009; 458:1131-5; PMID:19339967; http://dx.doi.org/10.1038/nature07976
13. Chittur SV, Sangster-Guity N, McCormick PJ. Histone deacetylase inhibitors: a new mode for inhibition of cholesterol metabolism. BMC Genomics 2008; 9:507; PMID:18959802; http://dx.doi.org/10.1186/1471-2164-9-507
14. Franck N, Gummesson A, Jernås M, Glad C, Svensson PA, Guillot G, Rudemo M, Nyström FH, Carlsson LM, Olsson B. Identification of adipocyte genes regulated by caloric intake. J Clin Endocrinol Metab 2011; 96:E413-8; PMID:21047925; http://dx.doi.org/10.1210/jc.2009-2534
15. Lanford RE, Guerra B, Lee H, Chavez D, Brasky KM, Bigger CB. Genomic response to interferon-alpha in chimpanzees: implications of rapid downregulation for hepatitis C kinetics. Hepatology 2006; 43:961-72; PMID:16628626; http://dx.doi.org/10.1002/hep.21167
16. Nguyen H, Sankaran S, Dandekar S. Hepatitis C virus core protein induces expression of genes regulating immune evasion and anti-apoptosis in hepatocytes. Virology 2006; 354:58-68; PMID:16876223; http://dx.doi.org/10.1016/j.virol.2006.04.028
17. Sawada H, Takami K, Asahi S. A toxicogenomic approach to drug-induced phospholipidosis: analysis of its induction mechanism and establishment of a novel in vitro screening system. Toxicol Sci 2005; 83:282-92; PMID:15342952; http://dx.doi.org/10.1093/toxsci/kfh264
18. Saftig P, Klumperman J. Lysosome biogenesis and lysosomal membrane proteins: trafficking meets function. Nat Rev Mol Cell Biol 2009; 10:623-35; PMID:19672277; http://dx.doi.org/10.1038/nrm2745
19. Chou HF, Passage M, Jonas AJ. Regulation of lysosomal sulfate transport by thyroid hormone. J Biol Chem 1994; 269:23524-9; PMID:8089119
20. DeMartino GN, Goldberg AL. Thyroid hormones control lysosomal enzyme activities in liver and skeletal muscle. Proc Natl Acad Sci U S A 1978; 75:1369-73; PMID:274725; http://dx.doi.org/10.1073/pnas.75.3.1369
21. Wu SM, Huang YH, Yeh CT, Tsai MM, Liao CH, Cheng WL, Chen WJ, Lin KH. Cathepsin H regulated by the thyroid hormone receptors associate with tumor invasion in human hepatoma cells. Oncogene 2011; 30:2057-69; PMID:21217776; http://dx.doi.org/10.1038/onc.2010.585
22. Monteforte R, Santillo A, Lanni A, D'Aniello S, Baccari GC. Morphological and biochemical changes in the Harderian gland of hypothyroid rats. J Exp Biol 2008; 211:606-12; PMID:18245638; http://dx.doi.org/10.1242/jeb.015115
23. Ke PY, Chen SS. Activation of the unfolded protein response and autophagy after hepatitis C virus infection suppresses innate antiviral immunity in vitro. J Clin Invest 2011; 121:37-56; PMID:21135505; http://dx.doi.org/10.1172/JCI41474
24. Kimura S, Noda T, Yoshimori T. Dissection of the autophagosome maturation process by a novel reporter protein, tandem fluorescent-tagged LC3. Autophagy 2007; 3:452-60; PMID:17534139
25. Huotari J, Helenius A. Endosome maturation. EMBO J 2011; 30:3481-500; PMID:21878991; http://dx.doi.org/10.1038/emboj.2011.286
26. Sinha RA, You SH, Zhou J, Siddique MM, Bay BH, Zhu X, Privalsky ML, Cheng SY, Stevens RD, Summers SA, et al. Thyroid hormone stimulates hepatic lipid catabolism via activation of autophagy. J Clin Invest 2012; 122:2428-38; PMID:22684107; http://dx.doi.org/10.1172/JCI60580
27. Kim J, Klionsky DJ. Autophagy, cytoplasm-to-vacuole targeting pathway, and pexophagy in yeast and mammalian cells. Annu Rev Biochem 2000; 69:303-42; PMID:10966461; http://dx.doi.org/10.1146/annurev.biochem.69.1.303
28. Huynh KK, Eskelinen EL, Scott CC, Malevanets A, Saftig P, Grinstein S. LAMP proteins are required for fusion of lysosomes with phagosomes. EMBO J 2007; 26:313-24; PMID:17245426; http://dx.doi.org/10.1038/sj.emboj.7601511

29. Blommaart EF, Luiken JJ, Blommaart PJ, van Woerkom GM, Meijer AJ. Phosphorylation of ribosomal protein S6 is inhibitory for autophagy in isolated rat hepatocytes. J Biol Chem 1995; 270:2320-6; PMID:7836465; http://dx.doi.org/10.1074/jbc.270.5.2320
30. Pattingre S, Espert L, Biard-Piechaczyk M, Codogno P. Regulation of macroautophagy by mTOR and Beclin 1 complexes. Biochimie 2008; 90:313-23; PMID:17928127; http://dx.doi.org/10.1016/j.biochi.2007.08.014
31. Molitoris JK, McColl KS, Swerdlow S, Matsuyama M, Lam M, Finkel TH, Matsuyama S, Distelhorst CW. Glucocorticoid elevation of dexamethasone-induced gene 2 (Dig2/RTP801/REDD1) protein mediates autophagy in lymphocytes. J Biol Chem 2011; 286:30181-9; PMID:21733849; http://dx.doi.org/10.1074/jbc.M111.245423
32. Xia X, Kar R, Gluhak-Heinrich J, Yao W, Lane NE, Bonewald LF, Biswas SK, Lo WK, Jiang JX. Glucocorticoid-induced autophagy in osteocytes. J Bone Miner Res 2010; 25:2479-88; PMID:20564240; http://dx.doi.org/10.1002/jbmr.160
33. Sobolewska A, Gajewska M, Zarzyńska J, Gajkowska B, Motyl T. IGF-I, EGF, and sex steroids regulate autophagy in bovine mammary epithelial cells via the mTOR pathway. Eur J Cell Biol 2009; 88:117-30; PMID:19013662; http://dx.doi.org/10.1016/j.ejcb.2008.09.004
34. Rusten TE, Lindmo K, Juhász G, Sass M, Seglen PO, Brech A, Stenmark H. Programmed autophagy in the *Drosophila* fat body is induced by ecdysone through regulation of the PI3K pathway. Dev Cell 2004; 7:179-92; PMID:15296715; http://dx.doi.org/10.1016/j.devcel.2004.07.005
35. Kuzman JA, O'Connell TD, Gerdes AM. Rapamycin prevents thyroid hormone-induced cardiac hypertrophy. Endocrinology 2007; 148:3477-84; PMID:17395699; http://dx.doi.org/10.1210/en.2007-0099
36. Cao X, Kambe F, Moeller LC, Refetoff S, Seo H. Thyroid hormone induces rapid activation of Akt/protein kinase B-mammalian target of rapamycin-p70S6K cascade through phosphatidylinositol 3-kinase in human fibroblasts. Mol Endocrinol 2005; 19:102-12; PMID:15388791; http://dx.doi.org/10.1210/me.2004-0093
37. Kenessey A, Ojamaa K. Thyroid hormone stimulates protein synthesis in the cardiomyocyte by activating the Akt-mTOR and p70S6K pathways. J Biol Chem 2006; 281:20666-72; PMID:16717100; http://dx.doi.org/10.1074/jbc.M512671200
38. Gnoni GV, Rochira A, Leone A, Damiano F, Marsigliante S, Siculella L. 3,5,3'triiodo-L-thyronine induces SREBP-1 expression by non-genomic actions in human HEP G2 cells. J Cell Physiol 2012; 227:2388-97; PMID:21826653; http://dx.doi.org/10.1002/jcp.22974
39. Baumgartner BG, Orpinell M, Duran J, Ribas V, Burghardt HE, Bach D, Villar AV, Paz JC, González M, Camps M, et al. Identification of a novel modulator of thyroid hormone receptor-mediated action. PLoS One 2007; 2:e1183; PMID:18030323; http://dx.doi.org/10.1371/journal.pone.0001183
40. Malik IA, Baumgartner BG, Naz N, Sheikh N, Moriconi F, Ramadori G. Changes in gene expression of DOR and other thyroid hormone receptors in rat liver during acute-phase response. Cell Tissue Res 2010; 342:261-72; PMID:20949361; http://dx.doi.org/10.1007/s00441-010-1067-4
41. Mauvezin C, Orpinell M, Francis VA, Mansilla F, Duran J, Ribas V, Palacín M, Boya P, Teleman AA, Zorzano A. The nuclear cofactor DOR regulates autophagy in mammalian and *Drosophila* cells. EMBO Rep 2010; 11:37-44; PMID:20010805; http://dx.doi.org/10.1038/embor.2009.242
42. Virgin HW, Levine B. Autophagy genes in immunity. Nat Immunol 2009; 10:461-70; PMID:19381141; http://dx.doi.org/10.1038/ni.1726
43. Morissette G, Moreau E, C-Gaudreault R, Marceau F. Massive cell vacuolization induced by organic amines such as procainamide. J Pharmacol Exp Ther 2004; 310:395-406; PMID:15007104; http://dx.doi.org/10.1124/jpet.104.066084
44. Morselli E, Maiuri MC, Markaki M, Megalou E, Pasparaki A, Palikaras K, Criollo A, Galluzzi L, Malik SA, Vitale I, et al. Caloric restriction and resveratrol promote longevity through the Sirtuin-1-dependent induction of autophagy. Cell Death Dis 2010; 1:e10; PMID:21364612; http://dx.doi.org/10.1038/cddis.2009.8
45. Czaja MJ. Functions of autophagy in hepatic and pancreatic physiology and disease. Gastroenterology 2011; 140:1895-908; PMID:21530520; http://dx.doi.org/10.1053/j.gastro.2011.04.038
46. Cao DJ, Wang ZV, Battiprolu PK, Jiang N, Morales CR, Kong Y, Rothermel BA, Gillette TG, Hill JA. Histone deacetylase (HDAC) inhibitors attenuate cardiac hypertrophy by suppressing autophagy. Proc Natl Acad Sci U S A 2011; 108:4123-8; PMID:21367693; http://dx.doi.org/10.1073/pnas.1015081108
47. Samuels HH, Stanley F, Casanova J. Depletion of L-3,5,3′-triiodothyronine and L-thyroxine in euthyroid calf serum for use in cell culture studies of the action of thyroid hormone. Endocrinology 1979; 105:80-5; PMID:446419; http://dx.doi.org/10.1210/endo-105-1-80
48. Shih CH, Chen SL, Yen CC, Huang YH, Chen CD, Lee YS, Lin KH. Thyroid hormone receptor-dependent transcriptional regulation of fibrinogen and coagulation proteins. Endocrinology 2004; 145:2804-14; PMID:14977860; http://dx.doi.org/10.1210/en.2003-1372
49. Liao CH, Yeh SC, Huang YH, Chen RN, Tsai MM, Chen WJ, Chi HC, Tai PJ, Liao CJ, Wu SM, et al. Positive regulation of spondin 2 by thyroid hormone is associated with cell migration and invasion. Endocr Relat Cancer 2010; 17:99-111; PMID:19903741; http://dx.doi.org/10.1677/ERC-09-0050